# Different flavours of oxygen help quantify seasonal variations of the biological carbon pump in the Celtic Sea

Isabel Seguro[1]*, Alina D. Marca[1], Jamie D. Shutler[2] and Jan Kaiser[1]

[1]Centre for Ocean and Atmospheric Sciences, School of Environmental Sciences, University of East Anglia (UEA), Norwich, United Kingdom, [2]Centre for Geography and Environmental Science, College of Life and Environmental Sciences, University of Exeter, Penryn, United Kingdom

Shelf seas represent only 10% of the World's Ocean by area but support up to 30% of its primary production. There are few measurements of biological production at high spatial and temporal resolution in these physically and biologically dynamic systems. Here, we use dissolved oxygen to-argon ($O_2$/Ar) ratios and oxygen triple isotopes in $O_2$ ($^{16}O$, $^{17}O$, $^{18}O$) to estimate net community production, $N(O_2/Ar)$, and gross $O_2$ production, $G(^{17}O)$, in summer and autumn 2014 and spring and summer 2015 in the Celtic Sea, as part of the UK Shelf-Sea Biogeochemistry Programme. Surface $O_2$/Ar concentration ratios were measured continuously using a shipboard membrane inlet mass spectrometer. Additional depth profiles of $O_2$/Ar concentration ratios, $\delta(^{17}O)$ and $\delta(^{18}O)$ were measured in discrete water samples from hydrocasts. The data were combined with wind-speed based gas exchange parameterisations to calculate biological air-sea oxygen fluxes. These fluxes were corrected for diapycnal diffusion, entrainment, production below the mixed layer, and changes over time to derive $N(O_2/Ar)$ and $G(^{17}O)$. The Celtic Sea showed the highest $G(^{17}O)$ in summer 2014 (825 mmol $m^{-2}$ $d^{-1}$) and lowest during autumn 2014 (153 mmol $m^{-2}$ $d^{-1}$). $N(O_2/Ar)$ was highest in spring 2015 (43 mmol $m^{-2}$ $d^{-1}$), followed by summer 2014 (42 mmol $m^{-2}$ $d^{-1}$), with a minimum in autumn 2014 (−24 mmol $m^{-2}$ $d^{-1}$). Dividing the survey region into three hydrographically distinct areas (Celtic Deep, Central Celtic Sea and Shelf Edge), we found that Celtic Deep and Shelf Edge had higher $N(O_2/Ar)$ in summer (71 and 63 mmol $m^{-2}$ $d^{-1}$, respectively) than in spring (49 and 22 mmol $m^{-2}$ $d^{-1}$). This study shows regional differences in the metabolic balance within the same season, as well as higher net community production in summer than in spring in some areas and years. The seasonal patterns in biological production rates and the export efficiency (*f*-ratio) identified the importance of biology for supporting the Celtic Sea's ability to act as a net $CO_2$ sink. Our measurements thus help improve our understanding of the biological carbon pump in temperate shelf seas.

# Introduction

Europe's population is increasing in coastal areas and predicted to continue growing in the future (Neumann et al., 2015). Northwest European shelf seas are also of high importance for recreational, artisanal and industrial fisheries (Sharples et al., 2013). An increasing population leads to an expansion in land use, industry, shipping, and therefore carbon dioxide ($CO_2$) emissions and pollution. These pressures can directly affect the biological functioning of these coastal areas (e.g., changes in biological community composition) (Painting et al., 2017).

At the base of the shelf sea food web, phytoplankton provide key marine services like atmospheric $CO_2$ uptake and sustaining fisheries (Sharples et al., 2009; Sharples et al., 2013). Phytoplankton are responsible for marine primary production and thus play a key role in the global carbon cycle. A fraction of the fixed organic carbon sinks to the seabed, reducing the amount of $CO_2$ at the sea surface and enabling more $CO_2$ to be taken up from the atmosphere. Despite shelf seas covering only about 10% of the ocean by area, they are responsible for 30-50% of inorganic and >80% of organic carbon burial (Bauer et al., 2013). The northwest European shelf is also the interface between coastal zones and the Atlantic Ocean. Therefore, quantifying biological production is essential to understand its role in $CO_2$ uptake and carbon export to the shelf seabed or to Atlantic deep waters.

Photosynthetic phytoplankton activity is determined by a combination of biogeochemical variables (nutrients, light, turbulence, temperature, etc.) that change seasonally (Seguro et al., 2015). Climate change is expected to alter this seasonal cycle (Henson et al., 2013; Landschützer et al., 2018), but it is still uncertain how these changes would affect the global carbon cycle (Bopp and Le Quéré, 2013). It is therefore important to quantify and understand spatial and seasonal variations in biological production and to help predict the impacts of growing populations and climate change.

Temperate shelf sea areas have been sampled more often than the open ocean because of their economic and ecologic importance. Previous studies of biological production in the Celtic Sea with "traditional" methods do not agree well (Joint and Pomroy, 1983; Holligan et al., 1984; Joint et al., 1986; Rees et al., 1999; Joint and Groom, 2000; Joint et al., 2001; Robinson et al., 2009; Hickman et al., 2012; Poulton et al., 2014), in part because of the inherent differences of each method ($^{14}C$, $^{18}O$, $^{15}N$, fast repetition rate fluorometry (FRRF), chlorophyll $a$, etc.) and their known biases (e.g., artifacts associated with incubation) (Marra, 2009; Robinson et al., 2009), but also because these areas are heterogeneous dynamic systems that require higher temporal and spatial resolution than the open ocean and snapshot sampling usually fails to capture their variability (Seguro et al., 2019). While satellite observations provide high spatial and temporal coverage when there are no clouds, these observations are mostly limited to the sea surface layer. Moreover, algorithms used to estimate net biological production and carbon export from satellite images need to be validated with *in situ* measurements, but different ways of estimating biological production have large uncertainties associated with methodological artefacts, assumptions on photosynthetic quotients or integration times (Cullen, 2001; Robinson et al., 2009). Those uncertainties makes it more difficult to evaluate satellite data-based

approaches and limit our knowledge of primary production in shelf seas. Thus, our understanding of the inter-annual, seasonal and spatial variability of biological production in temperate shelf seas, like the Celtic Sea, is still incomplete. In the context of climate change, with increasing $CO_2$ and ocean warming (IPCC, 2021), understanding how physical parameters (e.g., temperature) affect biological production is needed for predicting the ecological and biogeochemical response on $CO_2$ uptake and subsequent $O_2$ release.

The method based on oxygen isotopes to measure gross production without incubation (Luz and Barkan, 2000) provide a unique opportunity to understand the variability of dynamics systems at unprecedent high spatial resolution. To our knowledge, this is the first study of seasonal productivity in the Celtic Sea using the concentrations of oxygen ($O_2$), its isotopologues, and argon (Ar) as biogeochemical tracers.

While $CO_2$ is consumed, $O_2$ is produced during photosynthesis, therefore $O_2$ concentration changes can be used to estimate biological $O_2$ production. $O_2$ concentrations are also affected by physical processes such as air-sea gas exchange and mixing. We can quantify net community production (gross production minus respiration) by measuring $O_2$ supersaturation and using argon as a tracer to separate physical and biological factors affecting $O_2$ supersaturations (Craig and Hayward, 1987; Kaiser et al., 2005). Moreover, the isotopic signature of photosynthetic $O_2$ is different from atmospheric $O_2$ (Thiemens et al., 1995; Luz and Barkan, 2005) the latter of which is absorbed by the water through gas exchange. This difference in signature is due to the anomalous enrichment of stratospheric $O_3$ in $^{17}O$ and $^{18}O$ and isotope exchange with $CO_2$, leading to a corresponding $^{17}O$ and $^{18}O$ depletion in atmospheric $O_2$, relative to photosynthetic $O_2$ (Luz and Barkan, 2000). Using the three oxygen isotopologues $^{16}O_2$, $^{16}O^{17}O$, and $^{16}O^{18}O$ together allows us to eliminate the influence of respiration and any associated isotope effect. These differences in isotopic signature make it possible to quantify gross biological production by measuring the isotopic composition of dissolved oxygen. Gross biological production and net community production can then be converted to carbon-based quantities using photosynthetic stoichiometric quotients (Laws, 1991; Marra, 2002).

The data presented here combine high frequency underway observations of $O_2/Ar$ supersaturation, $\Delta(O_2/Ar)$, and discrete samples for oxygen triple isotopes ($^{16}O$, $^{17}O$, $^{18}O$), providing estimates of seasonal net community production, $N(O_2/Ar)$, and gross biological $O_2$ production, $G(^{17}O)$. The budget calculations account for production in the euphotic zone, air-sea gas exchange, diapycnal mixing, temporal changes and entrainment. We investigated the regional differences in the metabolic balance, estimate export efficiency $f$ as $N(O_2/Ar)/G(^{17}O)$ ratio and respiration as $R = G(^{17}O) - N(O_2/Ar)$, and its relationship with temperature.

# Material and methods

## Study area

The temperate Celtic Sea is part of the northwest European shelf and adjoins the northeast Atlantic Ocean. Temperate seas are characterised by seasonal differences in temperature, wind speeds, and

irradiance. The spring bloom usually starts in April when the water column becomes stratified and lasts up to two months. During summer, the water column remains stratified. Autumn starts with deepening of the surface mixed layer due to changes in winds and heat fluxes, leading to a fully mixed water column in winter (Simpson and Sharples, 2012). The currents are spatially variable and considered weak compared with the adjacent areas of the European Shelf Sea, especially in spring and summer when the winds are weaker than in autumn and winter (Holt et al., 2001). We sampled during three seasons (two summers, one autumn and one spring) on RRS Discovery cruises DY026 in August 2014, DY018 in November 2014, DY029 in April 2015 and DY033 in July 2015 as part of the NERC Shelf-Sea Biogeochemistry (SSB) programme. Up to 14 stations were sampled on every cruise, following a similar cruise track. Not all the stations were sampled on every cruise, but at least 3 main stations called A (51° N 6° W), CCS (49.5° N 8.5° W) and CS2 (48.5° N 9.5° W) were. The main stations were binned with the nearby ones, dividing the Celtic Sea into three areas, representing inner, middle and outer shelf: Celtic Deep (CD; 51°–50° N 8°–6° W; 100 m seabed depth), Central Celtic Sea (CCS; 50°–49.3° N 8.8°–8° W; 150 m seabed depth) and Shelf Edge (SE; 49.3°–48° N 10–8.8° W; 200 m seabed depth), respectively (Table 1, Figure 1).

## Methods

Along-track $O_2/Ar$ ratios were determined using a shipboard membrane inlet mass spectrometer (MIMS) connected to the ship's

underway seawater (USW) intake. We also collected discrete samples for oxygen triple isotopes that were subsequently analysed with a dual-inlet isotope ratio mass spectrometer (IRMS Finnigan MAT 252) in the Stable Isotope Laboratory at UEA. Discrete samples were taken at six depths from Niskin bottles attached to a conductivity-temperature-depth (CTD) rosette water sampler.
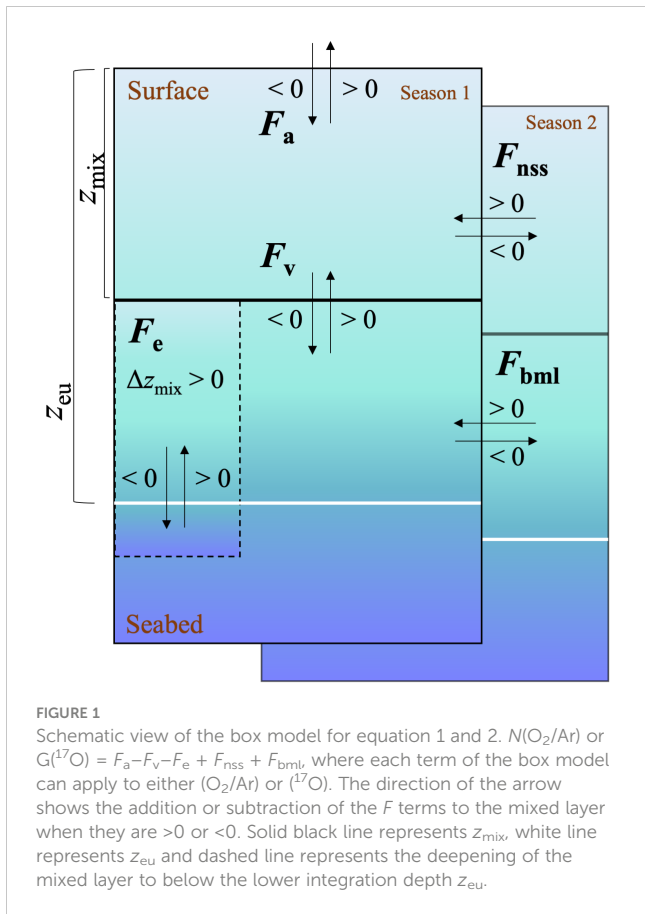
## Continuous measurements

Continuous $O_2/Ar$ ratio measurements were performed by MIMS. The MIMS was set-up according to Kaiser et al. (2005), with modifications detailed by Seguro et al. (2019). We calibrated the MIMS data with daily air-equilibrated water samples. On each cruise, at least one ship-transect passed the three areas Celtic Deep (stations A, J2, J3, J4, J5), Central Celtic Sea (stations CCS, J6, J7, J8) and Shelf Edge (stations CS2, Fe, O2, O4). USW data collection started in the English Channel and continued uninterrupted on all cruises, apart from cruise DY018 when the MIMS had an electronics fault. To compensate, discrete $O_2/Ar$ samples were taken every day from the USW and analysed by IRMS at UEA.

## Discrete measurements

Samples for the analysis of oxygen triple isotopes and $O_2/Ar$ were collected in evacuated 330 ml-glass flasks with high-vacuum

TABLE 1  Overview of data collected, mixed layer depth ($z_{mix}$), euphotic zone ($z_{eu}$) and stations (A, J2, J3, J4, J5, J6, J7, J8, CCS, O2, O4, CS2, Fe) at the three regions (Celtic Deep, Central Celtic Sea and Shelf Edge) with seabed depths (100 m, 150 m, 200 m) during the four cruises in autumn 2014, autumn 2015, spring 2015 and summer 2015.

| Cruise ID–Season | Number of hydrocasts | MIMS (days) | Celtic Deep (100 m) | Central Celtic Sea (150 m) | Shelf Edge (200 m) |
|---|---|---|---|---|---|
| DY026–Summer | 22 | 9 | A, J2 | CCS, J6 | CS2, Fe |
| 3–15 August 2014 | | | | | |
| $z_{mix}$/m | | | 20 | 19 | 15 |
| $z_{eu}$/m | | | 44 | 47 | 51 |
| DY018–Autumn | 23 | 0 | A, J2, J3, J5 | CCS, J6, J7, J8 | CS2, O2 |
| 9 November–3 December 2014 | | | | | |
| $z_{mix}$/m | | | 51 | 54 | 56 |
| $z_{eu}$/m | | | 50 | 50 | 77 |
| DY029–Spring | 34 | 28 | A, J2, J4 | CCS, J6 | CS2, Fe, O2, O4 |
| 1–30 April 2015 | | | | | |
| $z_{mix}$/m | | | 26 | 21 | 22 |
| $z_{eu}$/m | | | 32 | 29 | 52 |
| DY033–Summer | 24 | 21 | A, J2, J4 | CCS, J6 | CS2, Fe, O2, O4 |
| 11 July–3 August 2015 | | | | | |
| $z_{mix}$/m | | | 30 | 35 | 20 |
| $z_{eu}$/m | | | 53 | 62 | 67 |

**FIGURE 1**
Schematic view of the box model for equation 1 and 2. $N(O_2/Ar)$ or $G(^{17}O) = F_a - F_v - F_e + F_{nss} + F_{bml}$, where each term of the box model can apply to either $(O_2/Ar)$ or $(^{17}O)$. The direction of the arrow shows the addition or subtraction of the $F$ terms to the mixed layer when they are >0 or <0. Solid black line represents $z_{mix}$, white line represents $z_{eu}$ and dashed line represents the deepening of the mixed layer to below the lower integration depth $z_{eu}$.

stopcocks (Louwers Hapert), filled up to about 70% their volume, slightly below the optimum fill level (Seguro et al., 2019). The flasks contained 7 mg dry $HgCl_2$ to stop biological activity after sampling (Emerson et al., 1995). All samples were taken around midday to avoid bias due to diurnal variability. The standard deviation of $\Delta(O_2/Ar)$ duplicates was 0.1% or better. The standard deviation for dry air reference samples was 0.03 ‰ for $\delta(^{17}O)$, 0.06 ‰ for $\delta(^{18}O)$ and 8 ppm for the $^{17}O$ excess, defined as $^{17}\Delta = \delta(^{17}O) - 0.5179\,\delta(^{18}O)$ (Kaiser, 2011a), all with respect to $O_2$ in tropospheric air.

The *in situ* oxygen concentration, $c(O_2)$, was determined using a CTD-mounted oxygen sensor, calibrated against discrete samples analysed on board by automatic Winkler titration to a potentiometric endpoint (Culberson, 1991; Holley and Hydes, 1995).

## Net community and gross biological production calculation in the euphotic zone

To calculate net community production, $N(O_2/Ar)$, and gross production, $G(^{17}O)$, in the euphotic zone, we considered air-sea exchange fluxes ($F_a$), vertical diapycnal diffusion ($F_v$), entrainment due to mixed-layer depth changes ($F_e$) as well as non-steady state changes (temporal variations) in the mixed layer ($F_{nss}$) and in the euphotic zone below ($F_{bml}$) (Figure 1).

$$N(O_2/Ar) = F_a(O_2/Ar) - F_v(O_2/Ar) - F_e(O_2/Ar)$$
$$+ F_{nss}(O_2/Ar) + F_{bml}(O_2/Ar) \quad (1)$$

$$G(^{17}O) = F_a(^{17}O) - F_v(^{17}O) - F_e(^{17}O) + F_{nss}(^{17}O)$$
$$+ F_{bml}(^{17}O) \quad (2)$$

as described in the following paragraphs. The bottom of the euphotic zone ($z_{eu}$) was chosen as lower integration depth and was determined to be the depth corresponding to 1% of incident light using a PAR sensor mounted to the CTD (PAR: photosynthetically active radiation). All the terms on the right side of the equation adds to the mixed layer budget when > 0, apart from the $F_a$ term that is defined by convention as negative when entering in the ocean from the atmosphere (Figure 1).

### Air-sea exchange fluxes ($F_a$)

$\Delta(O_2/Ar)$ reflects the influence of biological processes (production and respiration of oxygen) (Craig and Hayward, 1987). $\Delta(O_2/Ar)$ is not significantly affected by physical processes such bubble injection and exchange because of the similar solubility and diffusivity of $O_2$ and Ar. $\Delta(O_2/Ar)$ together with the gas exchange coefficient $k(O_2)$ (Nightingale et al., 2000) and the oxygen saturation concentration $c_{sat}(O_2)$ (García and Gordon, 1992; Hamme and Emerson, 2004) can be used to calculate the biological $O_2$ air-sea exchange flux $F_a(O_2/Ar)$:

$$F_a(O_2/Ar) = k(O_2)c_{sat}(O_2)\Delta(O_2/Ar)$$
$$+ k(O_2)c_{sat}(O_2)[\Delta(O_2) - \Delta(O_2/Ar)]\sqrt{1 - \frac{Sc(O_2)}{Sc(Ar)}}$$
$$(3)$$

Sometimes, only the first term of Eq. 3 is used for the biological $O_2$ air-sea exchange flux and designated $F_{bio}$, but here we use the full expression $F_a(O_2/Ar)$ (Kaiser et al., 2005; Seguro et al., 2019) The second term in $F_a$ arises from small differences in the Schmidt numbers $Sc$ of $O_2$ and Ar. It is generally $\ll 0.1F_a$ and therefore often neglected.

Oxygen triple isotopes samples were used to estimate gross production *via* the dual delta method (Kaiser, 2011a; Kaiser and Abe, 2012), which avoids approximations and accounts for kinetic fractionation during invasion and evasion at the air-sea interface. Parameters used are as follows: $^{18}\varepsilon = -2.095$ ‰ and $^{17}\varepsilon = -1.082$ ‰ for the $^{18}O/^{16}O$ and $^{17}O/^{16}O$ kinetic isotope fractionations during $O_2$ evasion (Knox et al., 1992; Kaiser, 2011a); $\delta_{sat}$ for the isotope delta value of dissolved $O_2$ in equilibrium with the atmosphere at the measured temperature and salinity (Benson and Krause, 1984; Luz and Barkan, 2009), $\gamma = {}^{17}\varepsilon_R/{}^{18}\varepsilon_R = 0.5179$ for the ratio of the $^{17}O/^{16}O$ and $^{18}O/^{16}O$ respiration fractionations (Luz and Barkan, 2005); $^{17}\delta_P = -11.644$ ‰ and $^{18}\delta_P = -22.832$ ‰ for the isotope deltas of photosynthetic $O_2$ with respect to tropospheric $O_2$ (Kaiser, 2011a; Kaiser, 2011b; Kaiser and Abe, 2012).

$$F_a(^{17}O) = k(O_2)c_{sat}(O_2)\frac{(1 + {}^{17}\varepsilon)\frac{{}^{17}\delta - {}^{17}\delta_{sat}}{1 + {}^{17}\delta} - \gamma(1 + {}^{18}\varepsilon)\frac{{}^{18}\delta - {}^{18}\delta_{sat}}{1 + {}^{18}\delta} + s({}^{17}\varepsilon - \gamma{}^{18}\varepsilon)}{\frac{{}^{17}\delta_P - {}^{17}\delta}{1 + {}^{17}\delta} - \gamma\frac{{}^{18}\delta_P - {}^{18}\delta}{1 + {}^{18}\delta}}$$
$$(4)$$

## Vertical diapycnal diffusion ($F_v$)

$F_{vs}$ is calculated using a vertical eddy-diffusion coefficient of $K_z = (3 \pm 2) \times 10^{-5}\ \text{m}^2\ \text{s}^{-1}$ (Osborn, 1980; Simpson and Sharples, 2012; Palmer et al., 2013) and the $O_2/Ar$ concentration gradients evaluated at the bottom of the euphotic zone (Castro-Morales et al., 2013; Seguro et al., 2019)

$$F_v(O_2/Ar) = K_z c_{mix}(O_2)\ \mathrm{d}\ln[(c(O_2)/c(Ar)]/\mathrm{d}z \qquad (5)$$

where $c_{mix}(O_2)$ is the mixed-layer $O_2$ concentration.

Similarly, the diapycnal diffusion influence on $G(^{17}O)$ is calculated as (Seguro et al., 2019):

$$F_v(^{17}O) = K_z c_{mix}(O_2) \frac{\frac{\mathrm{d}\ln\left[\frac{1+^{17}\delta}{(1+^{18}\delta)^\gamma}\right]}{\mathrm{d}z}}{\frac{^{17}\delta_p - ^{17}\delta}{1+^{17}\delta} - \gamma \frac{^{18}\delta_p - ^{18}\delta}{1+^{18}\delta}} \qquad (6)$$

## Entrainment ($F_e$)

Entrainment of water below the mixed layer depth ($z_{mix}$) affects $N(O_2/Ar)$ and $G(^{17}O)$ when the mixed layer deepens ($\Delta z_{mix} > 0$) to below the lower integration depth $z_{eu}$, i.e., $z_{mix} + \Delta z_{mix} > z_{eu}$. $\Delta t$ is the number of days elapsed between the dates $\Delta z_{mix}$ has been determined. Following Castro-Morales et al. (2013) and Seguro et al. (2019) the resulting fluxes are

$$F_e(O_2/Ar) = 0.5 c_{mix}(O_2)\ (\Delta z_{mix})^2 / \Delta t\, \mathrm{d}\ln[c(O_2)/c(Ar)]/\mathrm{d}z \quad (7)$$

$$F_e(^{17}O) = 0.5 c_{mix}(O_2)(\Delta z_{mix})^2 / \Delta t \frac{\frac{\mathrm{d}\ln\left[\frac{1+^{17}\delta}{(1+^{18}\delta)^\gamma}\right]}{\mathrm{d}z}}{\frac{^{17}\delta_p - ^{17}\delta}{1+^{17}\delta} - \gamma \frac{^{18}\delta_p - ^{18}\delta}{1+^{18}\delta}} \qquad (8)$$

## Temporal changes ($F_{nss}$)

$F_{nss}$ can be estimated from samples taken at the same place at different times (e.g., 24 h or more apart) (Seguro et al., 2019). In this case, calculated as changes between seasons for the same area sampled.

$$F_{nss}(O_2/Ar) = z_{mix} c_{mix}(O_2)\mathrm{d}\ln[c(O_2)/c(Ar)]/\mathrm{d}t \qquad (9)$$

$$F_{nss}(^{17}O) = z_{mix} c_{mix}(O_2) \frac{\frac{\mathrm{d}\ln\left[\frac{1+^{17}\delta}{(1+^{18}\delta)^\gamma}\right]}{\mathrm{d}t}}{\frac{^{17}\delta_p - ^{17}\delta}{1+^{17}\delta} - \gamma \frac{^{18}\delta_p - ^{18}\delta}{1+^{18}\delta}} \qquad (10)$$

## Production below the mixed layer ($F_{bml}$)

is not affected by gas exchange and is only relevant at depths between $z_{mix}$ and the lower integration depth, $z_{eu}$. Because there is no exchange with the atmosphere below the mixed layer, we use $O_2$ values instead $O_2/Ar$.

$$F_{bml}(O_2/Ar) = F_{bml}(O_2) = \frac{\int_{z_{mix}}^{z_{eu}} c(O_2)\mathrm{d}z}{\mathrm{d}t} \qquad (11)$$

The isotopic composition below the mixed layer will change only due to biological processes, as it will not be affected by air exchange signal with time. The equation is the same as Eq. 10 but using $\delta$ values measured below the mixed layer (Luz and Barkan,

2009; Kaiser, 2011b).

$$F_{bml}(^{17}O) = (z_{eu} - z_{mix}) c_{bml}(O_2) \frac{\frac{\mathrm{d}\ln\left[\frac{1+^{17}\delta_{bml}}{(1+^{18}\delta_{bml})^\gamma}\right]}{\mathrm{d}t}}{\frac{^{17}\delta_p - ^{17}\delta}{1+^{17}\delta} - \gamma \frac{^{18}\delta_p - ^{18}\delta}{1+^{18}\delta}} \qquad (12)$$

Our estimates do not include horizontal advection because the sampling pattern did not allow us to obtain the required data. However, we expect that horizontal gradients perpendicular to the transect are relatively weak (Pingree and Le Cann, 1989). Also, advection is likely dominated by tidal flows, with weak residual currents, (Brown et al., 2003; Sharples et al., 2013), making them less important for our estimates over longer timescales of weeks to months. Upwelling fluxes can also be neglected in the sampled area.

## Metabolic efficiency

The combination of net community production and gross production allow us to calculate the metabolic efficiency of the biological pump, $f(O_2) = N(O_2/Ar)/G(^{17}O)$, an estimate of the part of gross production available for export (Laws et al., 2000; Haskell et al., 2017; Seguro et al., 2019). Values > 0 indicate net autotrophy (spring and summer); values < 0 net heterotrophy (autumn). Since we do not always have estimates of all terms in the budget for $N(O_2/Ar)$ and $G(^{17}O)$ (from equations 1 and 2), we also define $f_a(O_2) = F_a(O_2/Ar)/F_a(^{17}O)$ (from equations 3 and 4) as a proxy for the metabolic efficiency of the mixed layer only.

## Results

## Seasonal cycle of surface $\Delta(O_2/Ar)$ and biological fluxes

Discrete and continuous $O_2/Ar$ measurements were carried out on cruises DY026, DY029, and DY033; discrete ones only on cruise DY018. All cruises followed similar transects. Summer 2014 (DY026) and summer 2015 (DY033) showed net autotrophic conditions with surface $\Delta(O_2/Ar) = (4 \pm 2)$ % and $(2 \pm 1)$ %, respectively (Figure 2). In autumn 2014 (DY018), $\Delta(O_2/Ar)$ was (–1 ± 1) %. The highest $\Delta(O_2/Ar)$ values were found in spring 2015 (DY029), with a mean of (6 ± 4) %. Persistently low $\Delta(O_2/Ar)$ was observed in the English Channel south of Lyme Bay, east of 4° W, with negative values in both summer 2014 and 2015 and values near equilibrium in spring. Sea-surface temperature (SST) satellite images (not shown) indicate a change in temperature in this area, which may be associated with a change of the physical and biogeochemical regime that could explain the lower $\Delta(O_2/Ar)$.

## Seasonal variations of $^{17}\Delta$ and $\Delta(O_2/Ar)$ in the water column

The Central Celtic Sea showed distinct vertical profiles of $^{17}\Delta$ and $\Delta(O_2/Ar)$ during each season (Figure 3). At beginning of autumn, the lowest $^{17}\Delta$ of 24 ppm is found near the surface,

increasing with depth. The highest surface values of 50 to 60 ppm occur in spring and summer. In spring, we observed a $^{17}\Delta$ decrease with depth, whereas in summer $^{17}\Delta$ formed a subsurface maximum (>100 ppm) below the mixed layer and rapidly decreased deeper down.

$\Delta(O_2/Ar)$ values generally decrease with depth during all seasons, except for a summer subsurface maximum that coincides with the $^{17}\Delta$ maximum. Surface $\Delta(O_2/Ar)$ is > 5% spring, 1–2% in summer and< 0 in autumn.

## Net community production, gross production, and the efficiency of the biological pump

We calculated $G(^{17}O)$ and $N(O_2/Ar)$ for the whole of the Celtic Sea for each cruise. Mean values of the three areas in the Celtic Sea show the highest values of gross production in summer 2014 and summer 2015 (825 and 401 mmol m$^{-2}$ d$^{-1}$) and minima during autumn and spring (153 and 202 mmol m$^{-2}$ d$^{-1}$) (Table 2). Net community production was highest in spring 2015 and summer 2014 (43 and 42 mmol m$^{-2}$ d$^{-1}$), followed by summer 2015 (29 mmol m$^{-2}$ d$^{-1}$), and lowest in autumn (–24 mmol m$^{-2}$ d$^{-1}$). $G$($^{17}O$). Both $f(O_2)$ summer values (0.05 and 0.07) were lower than spring (0.21), and negative in autumn (–0.16), but all seasons showed significant variability across the sampling domain (Table 2).

To evaluate how gross and net community production vary regionally, mean $G(^{17}O)$ and $N(O_2/Ar)$ were calculated by dividing the Celtic Sea into three areas: Celtic Deep (CD), Central Celtic Sea (CCS), and Shelf Edge (SE) (Figure 2 and Tables 1, 3).

For CD, $G(^{17}O)$ was higher in summer (1282 and 532 mmol m$^{-2}$ d$^{-1}$ in 2014 and 2015, respectively) and lower in spring and autumn (184 and 212 mmol m$^{-2}$ d$^{-1}$). $F_a(^{17}O)$ dominated $G(^{17}O)$, with the other flux terms being mostly negligible, except for autumn when the mixed layer deepened, and $F_e(^{17}O)$ reached (50 mmol m$^{-2}$ d$^{-1}$). $F_v$($^{17}O$) was higher in summer (35 and 62 mmol m$^{-2}$ d$^{-1}$ in 2014 and 2015, respectively), while $F_{bml}(^{17}O)$ was higher in summer 2015 (45 mmol m$^{-2}$ d$^{-1}$) and negligible at other seasons.

Similar to $G(^{17}O)$, the air-sea exchange flux $F_a(O_2/Ar)$ dominated $N(O_2/Ar)$ at CD. $N(O_2/Ar)$ was higher in spring and summer (49 to 71 mmol m$^{-2}$ d$^{-1}$), with an autumn minimum of –45 mmol m$^{-2}$ d$^{-1}$. $F_v(O_2/Ar)$, $F_e(O_2/Ar)$, $F_{nss}(O_2/Ar)$, and $F_{bml}(O_2/Ar)$ all make minor contributions of –12 to +10 mmol m$^{-2}$ d$^{-1}$, corresponding to (0.2 ± 0.1) $F_a(O_2/Ar)$.

For CCS, $G(^{17}O)$ was smaller than for CD but still highest in summer (1007 and 310 mmol m$^{-2}$ d$^{-1}$ in 2014 and 2015, respectively) and lowest in autumn (16 mmol m$^{-2}$ d$^{-1}$). However, spring $G(^{17}O)$ was higher at CCS (254 mmol m$^{-2}$ d$^{-1}$) than at CD. Just as at CD, $F_a(^{17}O)$ generally approximates to $G(^{17}O)$, with the
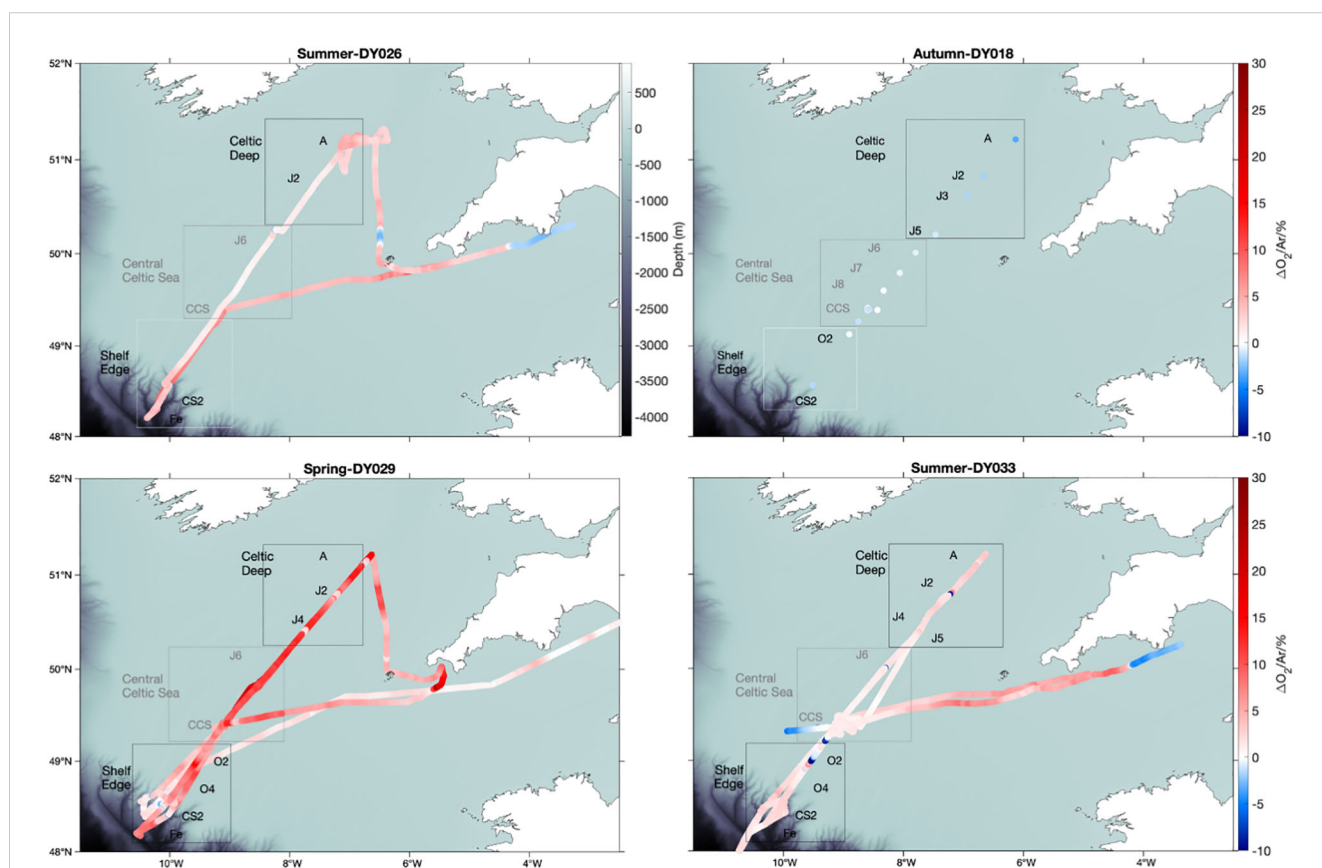


FIGURE 2
USW $\Delta(O_2/Ar)$ analysed by MIMS in summer 2014 (DY026), summer 2015 (DY033), autumn 2014 (DY018) and spring 2015 (DY029). Red colour shows $\Delta(O_2/Ar) > 0$ and blue $\Delta(O_2/Ar)< 0$.
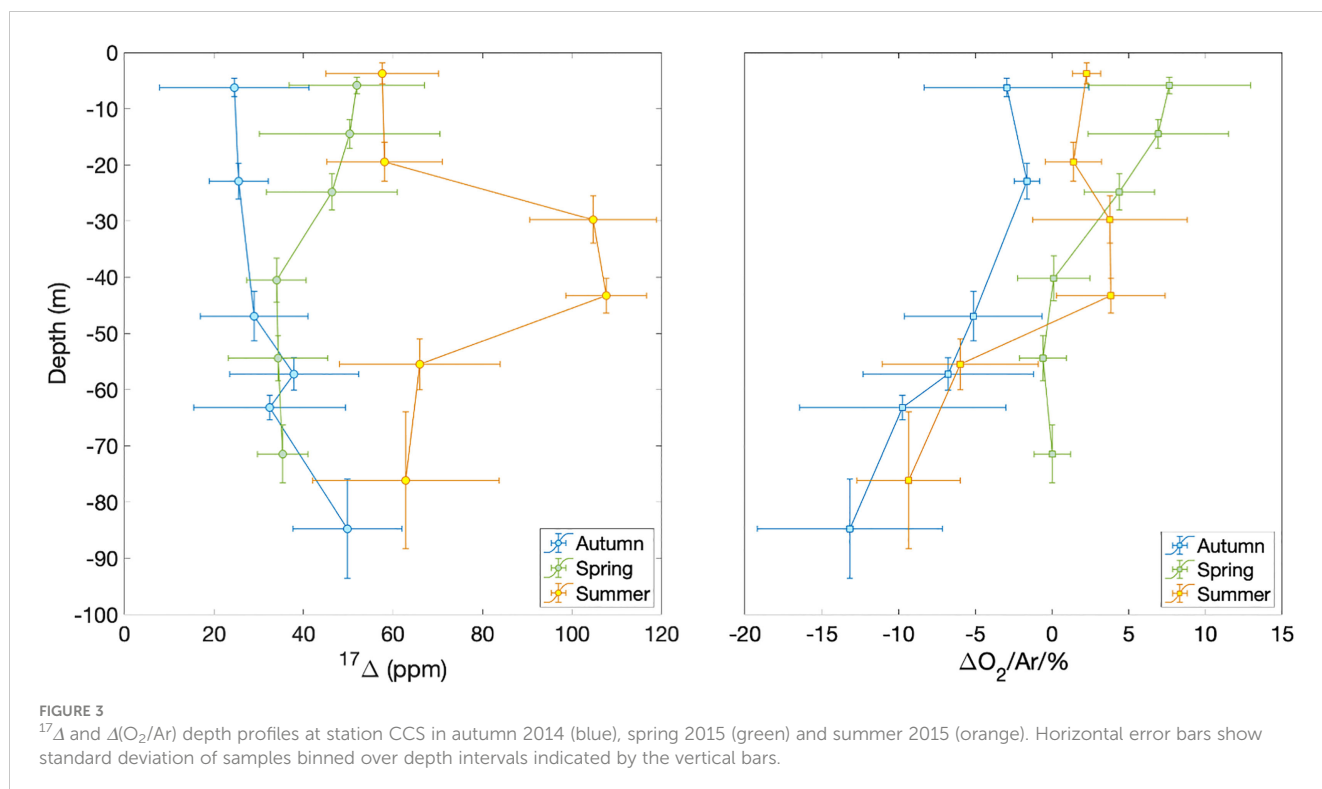
FIGURE 3

$^{17}\Delta$ and $\Delta(O_2/Ar)$ depth profiles at station CCS in autumn 2014 (blue), spring 2015 (green) and summer 2015 (orange). Horizontal error bars show standard deviation of samples binned over depth intervals indicated by the vertical bars.

other flux terms being negligible except for autumn. In summer 2015, $F_{bml}(^{17}O)$ made significant (44 mmol m$^{-2}$ d$^{-1}$), albeit minor, contribution.

The highest $N(O_2/Ar)$ at CCS occurred in spring (51 mmol m$^{-2}$ d$^{-1}$), while both summers were low (18 and 9 mmol m$^{-2}$ d$^{-1}$) and autumn was negative (−14 mmol m$^{-2}$ d$^{-1}$). In general, $F_e$, $F_{nss}$, and $F_{bml}$ showed the same patterns at CCS as at CD.

For SE, $G(^{17}O)$ was similar in all the seasons (from 169 to 360 mmol m$^{-2}$ d$^{-1}$) and dominated by $F_a(^{17}O)$. $F_v(^{17}O)$ was highest absolute value in summer (−23 mmol m$^{-2}$ d$^{-1}$) and negligible in autumn. $F_e(^{17}O)$ was only relevant in autumn (as at CD and CCS). $F_{nss}(^{17}O)$ and $F_{bml}(^{17}O)$ were negative in autumn (−29 and −44 mmol m$^{-2}$ d$^{-1}$, respectively) and positive in spring and summer, with a maximum $F_{bml}(^{17}O)$ of 61 mmol m$^{-2}$ d$^{-1}$ in summer 2015, but still<0.2 $F_a(^{17}O)$.

Summer 2014 $N(O_2/Ar)$ was the highest of all regions and seasons at SE (63 mmol m$^{-2}$ d$^{-1}$). In spring, $N(O_2/Ar)$ was the lowest of the three regions (22 mmol m$^{-2}$ d$^{-1}$). In autumn, $N(O_2/Ar)$ was equally low to CCS (−14 mmol m$^{-2}$ d$^{-1}$). $F_v(O_2/Ar)$ was mostly negligible except for summer 2014 (−14 mmol m$^{-2}$ d$^{-1}$). $F_e(O_2/Ar)$ was not significant. $F_{nss}(O_2/Ar)$ amounted to 0.2 $F_a(O_2/Ar)$

in autumn but was negligible in the other seasons. $F_{bml}(O_2/Ar)$ had a maximum in spring (8 mmol m$^{-2}$ d$^{-1}$) and a minimum in summer 2015 (−5 mmol m$^{-2}$ d$^{-1}$).

These results show that the non-$F_a$ terms, which are often neglected in open-ocean applications, can make significant, if generally minor, contributions to gross and net community production in the Celtic Sea. The relative influences of the non-$F_a$ terms are largest in autumn and are often non-negligible then. In summer, production below the mixed layer ($F_{bml}$) and diapycnal diffusion ($F_v$) can also be relevant.

To test whether metabolic efficiency and therefore carbon export could be parameterised in terms of a more readily measured variable, we plotted mixed-layer metabolic efficiency $f_a$($O_2$) against sea surface temperature $\vartheta$ (Figure 4). Our dataset contains only one season, autumn, at specific conditions of heterotrophy (and therefore no carbon available for export), mixed water column, as well as a narrow temperature range (12.5–14 °C). Therefore, we excluded the autumn data and investigated $f_a$($O_2$) and $\vartheta$ relationship under net autotrophic conditions only. While the relationship between $f_a$($O_2$) and $\vartheta$ does not seem to be very regionally, it is clearly clustered by seasons. The

TABLE 2  Average gross O$_2$ production $G(^{17}O)$ and net community O$_2$ production $N(O_2/Ar)$, by season.

| | $G(^{17}O)$/mmol m$^{-2}$ d$^{-1}$ | $N(O_2/Ar)$/mmol m$^{-2}$ d$^{-1}$ | $f(O_2)$ |
|---|---|---|---|
| Summer 2014 | 825 ± 570 | 42 ± 23 | 0.05 ± 0.04 |
| Autumn 2014 | 153 ± 119 | −24 ± 17 | −0.16 ± 0.16 |
| Spring 2015 | 202 ± 46 | 43 ± 18 | 0.21 ± 0.10 |
| Summer 2015 | 401 ± 117 | 29 ± 33 | 0.07 ± 0.09 |

The $f$-ratio is defined as $f$ = N($O_2$/Ar)/G($^{17}$O). The ± values are 1$\sigma$ standard deviations reflecting the spatial variability across the domain (rather than measurement uncertainty).

TABLE 3 Seasonal variations of $G(^{17}O) = F_a(^{17}O) - F_v(^{17}O) - F_e(^{17}O) + F_{nss}(^{17}O) + F_{bml}(^{17}O)$ and $N(O_2/Ar) = F_a(O_2/Ar) - F_v(O_2/Ar) - F_e(O_2/Ar) + F_{nss}(O_2/Ar) + F_{bml}(O_2/Ar)$ for the Celtic Deep, Central Celtic Sea and Shelf Edge areas.

| | | $G(^{17}O)$ | $F_a$ | $-F_v$ | $-F_e$ | $F_{nss}$ | $F_{bml}$ | $N(O_2/Ar)$ | $F_a$ | $-F_v$ | $-F_e$ | $F_{nss}$ | $F_{bml}$ |
|---|---|---|---|---|---|---|---|---|---|---|---|---|---|
| | | (in mmol m$^{-2}$ d$^{-1}$) | | | | | | (in mmol m$^{-2}$ d$^{-1}$) | | | | | |
| Celtic | Summer 2014 | **1282** | 1317 | −35 | | | | **41** | 45 | −4 | | | |
| Deep | Autumn 2014 | **212** | 297 | −10 | −50 | −21 | −4 | **−45** | −38 | 5 | −6 | −12 | 5 |
| | Spring 2015 | **184** | 170 | 6 | | 11 | −3 | **49** | 38 | 4 | | 6 | 2 |
| | Summer 2015 | **532** | 550 | −62 | 0 | −1 | 45 | **71** | 67 | −4 | 0 | 10 | −2 |
| Central | Summer 2014 | **1007** | 1021 | −14 | | | | **18** | 23 | −5 | | | |
| Celtic | Autumn 2014 | **16** | 117 | −30 | −25 | −33 | −13 | **-14** | −3 | 10 | −8 | −8 | −4 |
| Sea | Spring 2015 | **254** | 236 | 4 | | 13 | 1 | **57** | 51 | 2 | | 2 | 3 |
| | Summer 2015 | **310** | 289 | −24 | 1 | −1 | 44 | **9** | 12 | −2 | 1 | 2 | −3 |
| Shelf | Summer 2014 | **186** | 195 | −9 | | | | **63** | 48 | 14 | | | |
| Edge | Autumn 2014 | **231** | 328 | 1 | −26 | −29 | −44 | **−14** | −11 | 2 | −1 | −2 | −2 |
| | Spring 2015 | **169** | 159 | 3 | | 3 | 4 | **22** | 13 | 2 | | 0 | 8 |
| | Summer 2015 | **360** | 318 | −23 | | 5 | 61 | **13** | 17 | 0 | | 1 | −5 |

Since $F_{nss}$ and $F_{bml}$ were calculated between seasons, there are no values for summer 2014.

lowest temperatures (9.5–12 °C) correspond to spring with the highest $f_a(O_2)$ values. The highest temperatures (15–18 °C) correspond to summer with positive, but lower than spring $f_a(O_2)$. The spring and summer values decrease with temperature following $f_a(O_2) = (-0.022 \pm 0.004)\ \vartheta/°C + 0.41 \pm 0.05$ ($n = 66$; $r^2 = 0.34$; $p < 10^{-6}$) (Figure 4). Such a parameterisation may also be useful for data interpolation purposes.

We also looked at the relationship between community respiration ($R$) and sea surface temperature $\vartheta$. Community respiration can be calculated as $R = G(^{17}O) - N(O_2/Ar)$ using the regionally and seasonally aggregated values in Table 3. However, because the number of thus available data points was only small ($n = 12$), we also calculated it from the mixed-layer air-sea exchange flux terms, i.e., using $R_a = F_a(^{17}O) - F_a(O_2/Ar)$, because–as described above–the $F_a$ terms dominated both $G(^{17}O)$ and $N(O_2/Ar)$. Both methods gave similar weak positive linear relationships with temperature (Figure 5): $R = (63 \pm 40)\ \vartheta/°C - (5.2 \pm 5.7) \times 10^3$ ($n = 12$; $r^2 = 0.20$; $p = 0.15$) and $R_a = (58 \pm 20)\ \vartheta/°C - (4.5 \pm 2.7) \times 10^3$ ($n = 86$; $r^2 = 0.10$; $p = 0.004$).

# Discussion

## Instantaneous signal of biological production in the water column

From the $\Delta(O_2/Ar)$ and $^{17}\Delta$ depth profiles, it is possible to get semi-quantitative diagnostic information about the biogeochemical processes occurring in the euphotic zone. In autumn, the water column was not fully mixed yet during the sampling time, but less stratified than in summer. The water column gets fully mixed in winter (Sharples et al., 2013). The $^{17}\Delta$ increase with depth in the

autumn profile suggests ventilation bringing the $^{17}\Delta$ signal closer to the equilibrium value with air (Luz and Barkan, 2000). At the same time, $^{17}\Delta$ below the mixed layer is higher than at the surface because of the absence of air-sea gas exchange and the gross production signal, typically formed in the deep chlorophyll maximum during summer, remaining "trapped" below the mixed layer (Supplementary Material 1). This gross production in deeper layers is possible when the euphotic zone is deep enough to permit photosynthesis (e.g., nutrient-replete below the mixed layer and within the euphotic zone) (Supplementary Material 2). $\Delta(O_2/Ar)$ tells us how much of this biological oxygen remains in the water column after respiration. In autumn, negative values of $\Delta(O_2/Ar)$ means that respiration is greater than production, and therefore showing heterotrophic conditions. The effect of respiration increases with depth because of the absence of surface ventilation and decreasing photosynthesis due to decreasing PAR. Therefore, $\Delta(O_2/Ar) < 0$ in the autumn water column may indicate net heterotrophy due to the decrease in photosynthesis but also due to mixing with cooler low-$O_2$ deep waters from outside the shelf (Sharples et al., 2013; Humphreys et al., 2019) that can also reduce $\Delta(O_2/Ar)$.

In spring, the water column is stratified, due to solar surface irradiance and weakening of wind stress. The spring bloom showed the highest surface $^{17}\Delta$ values. The $^{17}\Delta$ increase is the result of accumulating gross production signal due to winter nutrients that permit optimum conditions for the bloom. These can also be seen in the positive $\Delta(O_2/Ar)$ values that decrease as expected with depth due to decreasing PAR.

A subsurface chlorophyll $a$ (Chl $a$) concentration maximum (45 ± 5 m), or deep chlorophyll maximum (DCM), below the mixed layer (30 ± 10 m) was detected by the CTD fluorometer (Supplementary Material 1) and associated with the maximum
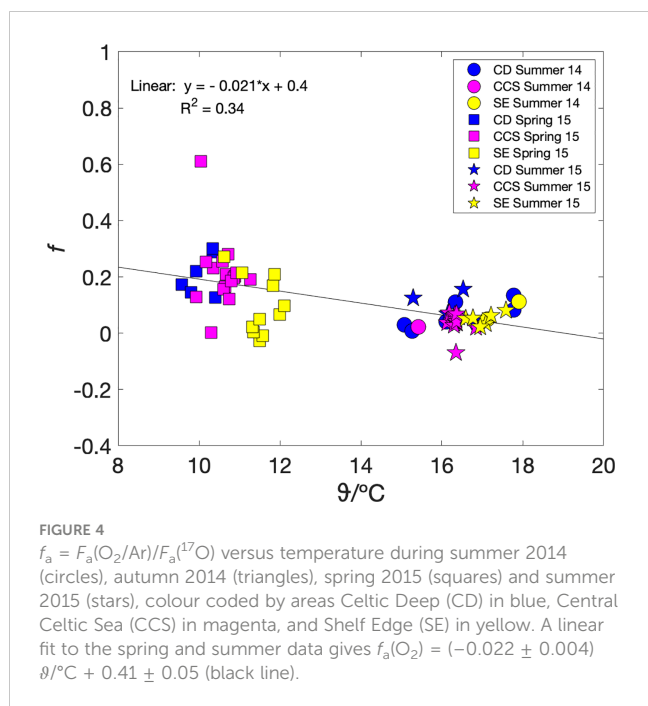
FIGURE 4
$f_a = F_a(O_2/Ar)/F_a(^{17}O)$ versus temperature during summer 2014 (circles), autumn 2014 (triangles), spring 2015 (squares) and summer 2015 (stars), colour coded by areas Celtic Deep (CD) in blue, Central Celtic Sea (CCS) in magenta, and Shelf Edge (SE) in yellow. A linear fit to the spring and summer data gives $f_a(O_2) = (-0.022 \pm 0.004)$ $\vartheta/°C + 0.41 \pm 0.05$ (black line).

$^{17}\Delta$ biological signal in summer. Surface (0–20 m) and deep (60–90 m) $^{17}\Delta$ values are of similar magnitude, only slightly lower in the surface due to ventilation (Wilhelm et al., 2004). Interestingly, respiration, calculated as $G(^{17}O)-N(O_2/Ar)$, was stronger in summer than in spring or even autumn, especially in the deeper layer. This was also found by Haskell et al. (2017) at the beginning of summer in the Southern California Bight, another coastal area. $\Delta(O_2/Ar)$ in summer was lower than in spring but still > 0 for much of the water column and< 0 below the DCM.
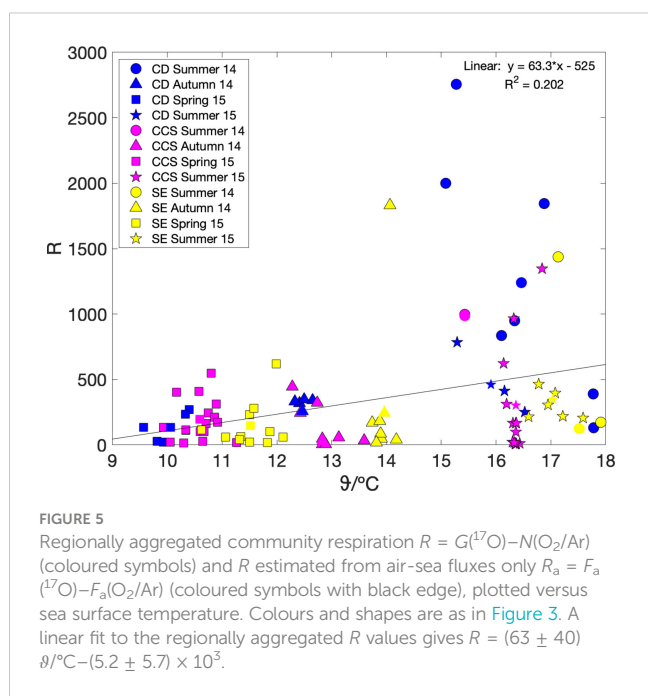


FIGURE 5
Regionally aggregated community respiration $R = G(^{17}O)-N(O_2/Ar)$ (coloured symbols) and $R$ estimated from air-sea fluxes only $R_a = F_a$ $(^{17}O)-F_a(O_2/Ar)$ (coloured symbols with black edge), plotted versus sea surface temperature. Colours and shapes are as in Figure 3. A linear fit to the regionally aggregated $R$ values gives $R = (63 \pm 40)$ $\vartheta/°C-(5.2 \pm 5.7) \times 10^3$.

## Seasonal and interannual production rate patterns and export

Gross production and net community production were both dominated by the air-sea exchange fluxes. While the other budget terms can quantitatively alter the calculated production rates, the general seasonal patterns seen in surface $^{17}\Delta$ and $\Delta(O_2/Ar)$ are conserved well. Including budget terms other than $F_a(O_2/Ar)$ and $F_a$ $(^{17}O)$ can make the calculations more accurate but reduces the spatial resolution (e.g., when calculating $F_{nss}$ from a revisited station). However, when logistically possible, (e.g., revisiting the same station two times or doing sampling from parallel platforms), biological production should include the whole euphotic zone when it is deeper than the mixed layer depth and account for vertical diapycnal diffusion, entrainment and non-steady state changes.

Additional uncertainty in the calculation of production comes from the lack of our ability to account for horizontal advection and current velocity. Again, this could be overcome by sampling from multiple platforms to estimate horizontal gradients and the use of mooring data to estimate mean advection velocities. Negative $F_e$ $(^{17}O)$, $F_{nss}(^{17}O)$, and $F_{bml}(^{17}O)$ mainly in the autumn season highlight the entrainment of different deep-water mass. Such negative values were also found by Haskell et al. (2017). In Haskell's study, the main reason for these negative values was entrainment, mixing and non-steady state transient changes over time. For the present study there are two plausible effects: 1) the influence of different water masses and 2) bias during sampling. The first hypothesis agrees with Haskell et al. (2017) as we also found entrainment of low-$\Delta(^{17}O)$ waters during autumn and summer. The second hypothesis applies specially to the summer sampling. The calculation of gross production below the mixed layer is challenging because, while any sample within the mixed layer should have the same $\Delta(^{17}O)$ value, samples taken below the mixed layer do not. A gradual decrease in Chl $a$ and oxygen concentrations from just below the mixed layer depth is normally seen in winter and spring profiles, but not in summer when a peak in Chl $a$ and oxygen below the mixed layer was found. This peak is not always constant with time and depth and can be only one or two meters thick. Discrete samples taken from 20 L-Niskin bottles collect water from a specific depth but at a resolution of about 2 m. That means that a high photosynthetic isotopic signal from thin layers may be missed by taking samples just one meter below the peak and therefore the measured values would be "diluted" by a low photosynthetic signal during the sampling process. These samples would still have a $^{17}\Delta$ value above equilibrium, but because the numerical methods used to calculate non-steady state terms, it can result in negative flux. For example, when calculating d$^{17}\Delta$/d$t$, if the first sample is taken at the subsurface maximum and the second sample has a lower value (but still > 0), the result will be a negative non-steady state term. In the case of entrainment, this is explained by a low $^{17}\Delta$ value diluting the mixed layer.

Looking at the $F_a(^{17}O)$ in different seasons and regions, we can say that the steady state assumption could be valid mainly in spring and summer but not in autumn, where $F_a(^{17}O)$ is overestimated by 40% for CD and SE, and six times higher for CCS. Similarly, $F_a(O_2/$

Ar) is a relatively good approximation of $N(O_2/Ar)$ if errors up to 20% are accepted, except for autumn when the other flux terms must also be considered.

A few studies have measured biological production in the Celtic Sea, which we have converted to $O_2$ equivalents here as per Seguro et al. (2019): Values ranged from 38 to 2400 mmol m$^{-2}$ d$^{-1}$ for gross production and 11-760 mmol m$^{-2}$ d$^{-1}$ for production using $^{14}$C, $^{13}$C, $^{18}$O, $O_2$ incubation methods and FRRF as in situ technique (Joint et al., 1986; Rees et al., 1999; Joint et al., 2001; Robinson et al., 2009; Hickman et al., 2012; Poulton et al., 2014). However, there were often methodological differences (e.g., the inclusion of heterotrophs or not, in situ vs incubation) and uncertainties from converting to $O_2$ equivalents make comparisons difficult (Juranek and Quay, 2013). Moreover, Robinson et al. (2009) made an exhaustive comparison of eight biological production estimation methods and found great discrepancies between them.

As far as we are aware, the only other publication on $G(^{17}O)$ and $N(O_2/Ar)$ measurements in the Celtic Sea is our own study (Seguro et al., 2019), which did not include the $F_{nss}(^{17}O)$ term of changes between seasons.

High-frequency underway observations of $\Delta(O_2/Ar)$ allowed us to see the heterogeneity of surface biological production during three different seasons and interannually for two summers. The two summers showed similar spatial patterns, with generally autotrophic conditions, but also values close to zero between 49.5° N and 51° N and even more consumption than oxygen production in the English Channel east of 4° W. Although the summer spatial patterns are similar in both years, $\Delta(O_2/Ar)$ in 2015 was half that of 2014. This is reflected in the mean $N(O_2/Ar)$ value and in $G(^{17}O)$, which is half in summer 2015 than 2014.

Net community production during the summer season is lower (42 mmol m$^{-2}$ d$^{-1}$ in 2014 and 29 mmol m$^{-2}$ d$^{-1}$ in 2015) than found in a previous study from 2011 in the Celtic Sea (63 to 180 mmol m$^{-2}$ d$^{-1}$) (Poulton et al., 2014).

On the other hand, our $G(^{17}O)$ is one order of magnitude higher (825 mmol m$^{-2}$ d$^{-1}$ in 2014 and 401 mmol m$^{-2}$ d$^{-1}$ in 2015) than $^{14}$C-based primary production measured in 2003 and 2005 (Hickman et al., 2012) (38 to 88 mmol m$^{-2}$ d$^{-1}$) for the summer season. These differences could be due to discrepancies between methods, since the $^{14}$C methods provides rates closer to net primary production (including autotrophic respiration), compared with $G(^{17}O)$, which includes any water-splitting, $O_2$-producing reaction. Clearly, interannual variability is also likely playing a role in causing these differences, e.g., in previous studies SST was (13.0 ± 0.5) °C, while it was (16.5 ± 0.5) °C for summer 2014 and 2015.

Parallel study estimated air-sea $CO_2$ fluxes at the CCS site during the spring bloom, they converted their data into oxygen net community production using photosynthetic quotient 1.4 and the values agreed well (Humphreys et al., 2019). Although we do not have winter data, our results follow the same pattern as the parallel $CO_2$ study that suggests the area of study is a net sink of atmospheric $CO_2$.

Interestingly, the metabolic efficiency of $f(O_2)$ does not differ much between the two summers in 2014 and 2015. Considering the whole Celtic Sea, this means that although gross production may change between years, planktonic respiration adjusts accordingly

and therefore the efficiency of the system is similar, but importantly not the absolute organic carbon export flux (or at least the potential for it). In contrast, autumn showed negative $f$ values, indicating that $O_2$ accumulated during summer was respired, and therefore there was no carbon available for export since organic matter was remineralised in the mixed layer. Spring had the highest $f(O_2)$ values, likely due to winter nutrient availability that permit optimum photosynthesis conditions.

Linear relationships between temperature and export production (Laws et al., 2000) as well as on respiration (Vázquez-Domínguez et al., 2007) has been previously investigated. We found a linear relationship between $f(O_2)$ and temperature that may provide a useful predictor for carbon export in this temperate shelf sea based on temperature only. Although our parameterisation may only apply to the Celtic Sea (e.g., nutrient availability in the area may be typically linked to seasonal temperature), other studies have found similar negative dependences of $f$ on temperature, e.g., –0.05 °C$^{-1}$ in a temperate coastal upwelling off the coast California (Haskell et al., 2017). Based on our results, an increase of sea surface temperature by 1°C would reduce export to deep waters by 2%. This suggests that future increases in temperature could cause a reduction in annual net carbon export. Although further observations would be needed to make this parameterisation more robust, these first findings may have major implications on our understanding on how shelf seas may change the efficiency of carbon export due to ocean warming.

The weak positive relationship between respiration and temperature we found for the Celtic Sea can hardly be called statistically significant, but qualitatively agrees with the Mediterranean Sea study of Vázquez-Domínguez et al. (2007). However, the effect of temperature alone in marine systems is complex and may not fully explain marine metabolism (Lawrence and William, 2001). Since different seas may have completely different community taxonomy, physical conditions and nutrient status, a single model to predict respiration rate change solely from temperature does not seem to be adequate. However, several studies showing relationships between temperature and export or respiration may help to predict the effect of local ocean warming.

## Conclusions

During the UK NERC Shelf-Sea Biogeochemistry Programme in 2014–15, spring and summer in the Celtic Sea were net autotrophic, while autumn was net heterotrophic. Although the sampling programme did not cover the whole year, the variability between seasons was well characterised, the two summer seasons showed similar production rates, plus the magnitude of the values measured suggests that the Celtic Sea is a net autotrophic system on an annual basis.

The number of samples and therefore the spatial resolution were reduced when including budget terms other than air-sea exchange fluxes in the calculations. Air-sea exchange fluxes ($F_a$) alone can deviate by up to six times from estimates that cover the whole of the euphotic zone and account for non-steady state inventory changes, entrainment, and vertical eddy diffusion,

depending on season and conditions. This highlights the need for high-resolution measurements in dynamic regions such as the Celtic Sea. Reducing the sampling protocol to snapshots may bias the biological production estimates in shelf seas. On the flip side, more comprehensive calculation frameworks entail higher overall uncertainty and widen the confidence intervals for the final values. Nevertheless, seasonal variability in respiration and metabolic efficiency are consistent regardless of the calculation used. After all, net community production is highest in spring and gross production is highest in summer. The whole Celtic Sea is net autotrophic during spring and summer, but in general decreases towards the outer shelf. The Celtic Sea shifts to net heterotrophic in autumn and shows higher respiration during summer. Hence, this study characterised the seasonal biological net and gross production rates, highlighting the importance of high-resolution measurements and showed that the biological pump helps support the Celtic Sea being a net carbon sink. Further studies in the Celtic Sea would benefit from similar temporal and spatial data coverage, to accurately understand the rates and efficiency of carbon export for the whole shelf and how global climate change may affect them.

## Data availability statement

The datasets presented in this study have been deposited with the British Oceanography Data Centre (BODC) and can be found under https://doi.org/10.5285/fab73b69-21b9-5ae8-e053-6c86abc0960c.

## Author contributions

IS, AM, JS, and JK designed the study and fieldwork. IS carried out the fieldwork and IS, AM, and JK the laboratory analyses. IS, JS, and JK contributed to processing the data. All authors contributed to the article and approved the submitted version.

## Funding

## Acknowledgments

## Conflict of interest

The authors declare that the research was conducted in the absence of any commercial or financial relationships that could be construed as a potential conflict of interest.

## Publisher's note

All claims expressed in this article are solely those of the authors and do not necessarily represent those of their affiliated organizations, or those of the publisher, the editors and the reviewers. Any product that may be evaluated in this article, or claim that may be made by its manufacturer, is not guaranteed or endorsed by the publisher.

## Supplementary material

The Supplementary Material for this article can be found online at: https://www.frontiersin.org/articles/10.3389/fmars.2023.1037470/full#supplementary-material

## References

Bauer, J. E., Cai, W.-J., Raymond, P. A., Bianchi, T. S., Hopkinson, C. S., and Regnier, P. A. G. (2013). The changing carbon cycle of the coastal ocean. *Nature* 504, 61–70. doi: 10.1038/nature12857

Benson, B. B., and Krause, D. (1984). The concentration and isotopic fractionation of oxygen dissolved in fresh water and seawater in equilibrium with the atmosphere. *Limnol. Oceanogr.* 29, 620–632. doi: 10.4319/lo.1984.29.3.0620

Bopp, L., and Le Quéré, C. (2013). "Ocean carbon cycle," In C. Le Quéré and E. S. Saltzman eds. *Surface ocean–lower atmosphere processes*. doi: 10.1029/2008GM000780

Brown, J., Carrillo, L., Fernand, L., Horsburgh, K. J., Hill, A. E., Young, E. F., et al. (2003). Observations of the physical structure and seasonal jet-like circulation of the celtic Sea and st. george's channel of the Irish Sea. *Continental Shelf Res.* 23, 533–561. doi: 10.1016/S0278-4343(03)00008-6

Castro-Morales, K., Cassar, N., Shoosmith, D. R., and Kaiser, J. (2013). Biological production in the bellingshausen Sea from oxygen-to-argon ratios and oxygen triple isotopes. *Biogeosciences* 10, 2273–2291. doi: 10.5194/bg-10-2273-2013

Craig, H., and Hayward, T. (1987). Oxygen supersaturation in the ocean: biological versus physical contributions. *Science* 235, 202–205. doi: 10.1126/science.235.4785.199

Culberson, C. H. (1991). *Dissolved oxygen, in WOCE Operations Manual - Part 3.1.3: WHP Operations and Methods*. WHP Office Report WHPO 91-1. WOCE Report No. 68/91. Revision 1, edited, Woods Hole. Massachusetts, USA.

Cullen, J. J. (2001). Primary production methods. In*Encyclopedia of Ocean Sciences* Halifax: Academic Press 4, 2277–2284. doi: 10.1006/rwos.2001.0203

Emerson, S., Quay, P. D., Stump, C., Wilbur, D., and Schudlich, R. (1995). Chemical tracers of productivity and respiration in the subtropical pacific ocean. *J. Geophys. Res.* 100, 15873. doi: 10.1029/95JC01333

García, H. E., and Gordon, L. I. (1992). Oxygen solubility in seawater: better fitting equations. *Limnol. Oceanogr.* 37, 1307–1312. doi: 10.4319/lo.1992.37.6.1307

Hamme, R. C., and Emerson, S. R. (2004). The solubility of neon, nitrogen and argon in distilled water and seawater. *Deep Sea Res. Part I: Oceanogr. Res. Pap.* 51, 1517–1528. doi: 10.1016/j.dsr.2004.06.009

Haskell, W. Z., Prokopenko, M. G., Hammond, D. E., Stanley, R. H. R., and Sandwith, Z. O. (2017). Annual cyclicity in export efficiency in the inner southern California bight. *Global Biogeochem. Cycles* 31, 357–376. doi: 10.1002/2016GB005561

Henson, S., Cole, H., Beaulieu, C., and Yool, A. (2013). The impact of global warming on seasonality of ocean primary production. *Biogeosciences* 10, 4357–4369. doi: 10.5194/bg-10-4357-2013

Hickman, A. E., Moore, C. M., Sharples, J., Lucas, M. I., Tilstone, G. H., Krivtsov, V., et al. (2012). Primary production and nitrate uptake within the seasonal thermocline of a stratified shelf sea. *Mar. Ecol. Prog. Ser.* 463, 39–57. doi: 10.3354/meps09836

Holley, S. E., and Hydes, D. J. (1995). Procedure for the determination of dissolved oxygen in seawater. *James Rennell Centre Ocean Circulation Internal Document* 20, 38.

Holligan, P., Leb, W. P., Purdie, D., and Harris, R. (1984). Photosynthesis, respiration and nitrogen supply of plankton populations in stratified, frontal and tidally mixed shelf waters. *Mar. ecol. Prog. Ser.* 17, 201–213. doi: 10.3354/meps017201

Holt, J. T., James, I. D., and Jones, J. E. (2001). An s coordinate density evolving model of the northwest European continental shelf: 2. seasonal currents and tides. *J. Geophys. Res.: Oceans* 106, 14035–14053. doi: 10.1029/2000JC000304

Humphreys, M. P., Achterberg, E. P., Hopkins, J. E., Chowdhury, M. Z. H., Griffiths, A. M., Hartman, S. E., et al. (2019). Mechanisms for a nutrient-conserving carbon pump in a seasonally stratified, temperate continental shelf sea. *Prog. Oceanogr.* 177, 101961. doi: 10.1016/j.pocean.2018.05.001

IPCC (2021). *Climate change 2021: the physical science basis. contribution of working group I to the sixth assessment report of the intergovernmental panel on climate change.* Eds. V. ,. P. Masson-Delmotte, A. Zhai, S. L. Pirani, C. Connors, S. Péan, N. Berger, Y. Caud, L. Chen, M. I. Goldfarb, M. Gomis, K. Huang, E. Leitzell, J. B. R. Lonnoy, T. K. Matthews, T. Maycock, O. Waterfield, R. Yelekçi, Yu, and B. Zhou (Cambridge, United Kingdom and New York, NY, USA: Cambridge University Press).

Joint, I., and Groom, S. B. (2000). Estimation of phytoplankton production from space: current status and future potential of satellite remote sensing. *J. Exp. Mar. Biol. Ecol.* 250, 233–255. doi: 10.1016/S0022-0981(00)00199-4

Joint, I. R., Owens, N. J. P., and Pomroy, A. J. (1986). Seasonal production of photosynthetic picoplankton and nanoplankton in the celtic Sea. *Mar. Ecol. Prog. Ser.* 28, 251–258. doi: 10.3354/meps028251

Joint, I. R., and Pomroy, A. J. (1983). Production of picoplankton and small nanoplankton in the celtic Sea. *Mar. Biol.* 77, 19–27. doi: 10.1007/BF00393206

Joint, I., Wollast, R., Chou, L., Batten, S., Elskens, M., Edwards, E., et al. (2001). Pelagic production at the celtic Sea shelf break. *Deep Sea Res. Part II: Topical Stud. Oceanogr.* 48, 3049–3081. doi: 10.1016/S0967-0645(01)00032-7

Juranek, L. W., and Quay, P. D. (2013). Using triple isotopes of dissolved oxygen to evaluate global marine productivity. *Annu. Rev. Mar. Sci.* 5, 503–524. doi: 10.1146/annurev-marine-121211-172430

Kaiser, J. (2011a). Corrigendum to "Technical note: consistent calculation of aquatic gross production from oxygen triple isotope measurements" published in biogeosciences, 8, 1793–1811, 2011. *Biogeosciences* 8, 2561–2565. doi: 10.5194/bg-8-1793-2011

Kaiser, J. (2011b). Technical note: consistent calculation of aquatic gross production from oxygen triple isotope measurements. *Biogeosciences* 8, 1793–1811.

Kaiser, J., and Abe, O. (2012). Reply to nicholson's comment on "Consistent calculation of aquatic gross production from oxygen triple isotope measurements" by kaiser, 2011). *Biogeosciences* 9, 2921–2933. doi: 10.5194/bg-9-2921-2012

Kaiser, J., Reuer, M. K., Barnett, B., and Bender, M. L. (2005). Marine productivity estimates from continuous O2/Ar ratio measurements by membrane inlet mass spectrometry. *Geophys. Res. Lett.* 32, L19605. doi: 10.1029/2005GL023459

Knox, M., Quay, P. D., and Wilbur, D. (1992). Kinetic isotopic fractionation during air-water gas transfer of O2, N2, CH4, and H2. *J. Geophys. Res.* 97, 20335. doi: 10.1029/92JC00949

Landschützer, P., Gruber, N., Bakker, D. C. E., Stemmler, I., and Six, K. D. (2018). Strengthening seasonal marine CO2 variations due to increasing atmospheric CO2. *Nat. Climate Change* 8, 146–150. doi: 10.1038/s41558-017-0057-x

Lawrence, R. P., and William, J. W. (2001). Temperature and substrates as interactive limiting factors for marine heterotrophic bacteria. *Aquat. Microbial. Ecol.* 23, 187–204. doi: 10.3354/ame023187

Laws, E. A. (1991). Photosynthetic quotients, new production and net community production in the open ocean. *Deep Sea Res. Part A. Oceanogr. Res. Pap.* 38, 143–167. doi: 10.1016/0198-0149(91)90059-O

Laws, E. A., Falkowski, P. G., Smith, W. O., Ducklow, H., and Mccarthy, J. J. (2000). Temperature effects on export production in the open ocean. *Global Biogeochem. Cycles* 14, 1231–1246. doi: 10.1029/1999GB001229

Luz, B., and Barkan, E. (2000). Assessment of oceanic productivity with the triple-isotope composition of dissolved oxygen. *Science* 288, 2028–2031. doi: 10.1126/science.288.5473.2028

Luz, B., and Barkan, E. (2005). The isotopic ratios $^{17}O/^{16}O$ and $^{18}O/^{16}O$ in molecular oxygen and their significance in biogeochemistry. *Geochim. Cosmochim. Acta* 69, 1099–1110. doi: 10.1016/j.gca.2004.09.001

Luz, B., and Barkan, E. (2009). Net and gross oxygen production from O2/Ar, $^{17}O/^{16}O$ and $^{18}O/^{16}O$ ratios. *Aquat. Microbial. Ecol.* 56, 133–145. doi: 10.3354/ame01296

Marra, J. (2002). Approaches to the measurement of plankton production. In P. J. L. B. Williams, D. N. Thomas and C. S. Reynolds eds. *Phytoplankton Productivity*, 78–108. doi: 10.1002/9780470995204.ch4

Marra, J. (2009). Net and gross productivity: weighing in with $^{14}C$. *Aquat. Microbial. Ecol.* 56, 123–131. doi: 10.3354/ame01306

Neumann, B., Vafeidis, A. T., Zimmermann, J., and Nicholls, R. J. (2015). Future coastal population growth and exposure to sea-level rise and coastal flooding–a global assessment. *PloS One* 10, e0118571. doi: 10.1371/journal.pone.0118571

Nightingale, P. D., Malin, G., Law, C. S., Watson, A. J., Liss, P. S., Liddicoat, M. I., et al. (2000). *In situ* Evaluation of air-sea gas exchange parameterizations using novel conservative and volatile tracers. *Global Biogeochem. Cycles* 14, 373–387. doi: 10.1029/1999GB900091

Osborn, T. R. (1980). Estimates of the local rate of vertical diffusion from dissipation measurements. *J. Phys. Oceanogr.* 10, 83–89. doi: 10.1175/1520-0485(1980)010<0083:EOTLRO>2.0.CO;2

Painting, S. J, Collingridge, K. A., Durand, D., Grémare, A., Créach, V., Arvanitidis, C., et al (2020). Marine monitoring in Europe: is it adequate to address environmental threats and pressures? *Ocean Science* 16, 235–252. doi: 10.5194/os-16-235-2020

Palmer, M. R., Inall, M. E., and Sharples, J. (2013). The physical oceanography of Jones bank: a mixing hotspot in the celtic Sea. *Prog. Oceanogr.* 117, 9–24. doi: 10.1016/j.pocean.2013.06.009

Pingree, R. D., and Le Cann, B. (1989). Celtic and armorican slope and shelf residual currents. *Prog. Oceanogr.* 23, 303–338. doi: 10.1016/0079-6611(89)90003-7

Poulton, A. J., Stinchcombe, M. C., Achterberg, E. P., Bakker, D. C. E., Dumousseaud, C., Lawson, H. E., et al. (2014). Coccolithophores on the north-west European shelf: calcification rates and environmental controls. *Biogeosciences* 11, 3919–3940. doi: 10.5194/bg-11-3919-2014

Rees, A. P., Joint, I., and Donald, K. M. (1999). Early spring bloom phytoplankton-nutrient dynamics at the celtic Sea shelf edge. *Deep Sea Res. Part I: Oceanogr. Res. Pap.* 46, 483–510. doi: 10.1016/S0967-0637(98)00073-9

Robinson, C., Tilstone, G. H., Rees, A. P., Smyth, T. J., Fishwick, J. R., Tarran, G. A., et al. (2009). Comparison of *in vitro* and *in situ* plankton production determinations. *Aquat. Microbial. Ecol.* 54, 13–34. doi: 10.3354/ame01250

Seguro, I., García, C. M., Papaspyrou, S., Gálvez, J. A., García-Robledo, E., Navarro, G., et al (2015). Seasonal changes of the microplankton community along a tropical estuary. *Regional Stud. Mar. Sci.* 2, 189–202. doi: 10.1016/j.rsma.2015.10.006

Seguro, I., Marca, A. D., Painting, S. J., Shutler, J. D., Suggett, D. J., and Kaiser, J. (2019). High-resolution net and gross biological production during a celtic Sea spring bloom. *Prog. Oceanogr.* 177, 101885. doi: 10.1016/j.pocean.2017.12.003

Sharples, J., Ellis, J. R., Nolan, G., and Scott, B. E. (2013). Fishing and the oceanography of a stratified shelf sea. *Prog. Oceanogr.* 117, 130–139. doi: 10.1016/j.pocean.2013.06.014

Sharples, J., Moore, C. M., Hickman, A. E., Holligan, P. M., Tweddle, J. F., Palmer, M. R., et al. (2009). Internal tidal mixing as a control on continental margin ecosystems. *Geophys. Res. Lett.* 36, L23603. doi: 10.1029/2009GL040683

Simpson, J. H., and Sharples, J. (2012). *Introduction to the physical and biological oceanography of shelf seas* (Cambridge: Cambridge University Press). doi: 10.1017/CBO9781139034098

Thiemens, M. H., Jackson, T., Zipf, E. C., Erdman, P. W., and Van Egmond, C. (1995). Carbon dioxide and oxygen isotope anomalies in the mesosphere and stratosphere. *Science* 270, 969–972. doi: 10.1126/science.270.5238.969

Vázquez-Domínguez, E., Vaqué, D., and Gasol, J. M. (2007). Ocean warming enhances respiration and carbon demand of coastal microbial plankton. *Global Change Biol.* 13, 1327–1334. doi: 10.1111/j.1365-2486.2007.01377.x

Wilhelm, C., Becker, A., Toepel, J., Vieler, A., and Rautenberger, R. (2004). Photophysiology and primary production of phytoplankton in freshwater. *Physiol. Plantarum* 120, 347–357. doi: 10.1111/j.0031-9317.2004.00267.x